J Therm Anal Calorim (2011) 105:811–821
DOI 10.1007/s10973-010-1167-0

Utilising thermoporometry to obtain new insights into nanostructured materials

Review part 1

Joakim Riikonen · Jarno Salonen · Vesa-Pekka Lehto

ESTAC2010 Conference Special Issue

Abstract Thermoporometry is a relatively new method of characterising porous properties of nanostructured materials based on observation of solid–liquid phase transitions of materials confined in pores. It provides several advantages over the conventional characterisation methods, mercury porosimetry and gas sorption. The advantages include possibility of using short measurement times, non-toxic chemicals and wet samples. In addition, complicated sample preparation and specialised instruments are not required. Therefore, it has a great potential of becoming a widely utilised characterisation method, although its potential has not yet been widely realised. In recent years, there has been a significant increase in research activities regarding the method. In the first part of the review, we introduce thermoporometry and review related results of the confinement effects on materials and their solid–liquid phase transition.

Keywords Thermoporometry · Mesoporous · Freezing · Melting · Characterisation

Introduction

Nanostructured materials have attracted substantial interest in many fields of science. Among the most interesting nanostructured materials are mesoporous materials which consist of voids, i.e. pores, ranging from 2 to 50 nm in diameter [1]. The number of publications related to mesoporous materials has been steadily rising since 1990's and currently there are thousands of research articles being published yearly (Fig. 1).

These materials have potential applications in various fields such as catalysis [2, 3], separation [2], electronics [4] and sensing [5, 6]. In recent years, emerging applications of mesoporous materials in the fields of drug delivery and medical diagnostics have been studied [7, 8]. It has been shown, for example, that mesoporous materials can be used in the delivery of peptides and poorly soluble drugs [9–11]. These applications utilise the unique properties of these materials such as large specific surface areas (up to 1,000 m^2/g), controllable pore size and homogenous structure [1, 12].

Ordered mesoporous silica and porous silicon (PSi) are one of the most studied mesoporous materials. Ordered mesoporous silica materials, such as MCM-41, SBA-15 and KIT-5, are bottom-up materials that exhibit well-ordered structures which can be controlled during synthesis [13–15]. Mesoporous silicon, on the other hand, is a top-down material, which is produced by electrochemical etching of a surface of silicon wafer, and exhibits various controllable structures [12].

Due to increasing use of mesoporous materials there is an increasing need for characterisation of mesoporous materials. There are few methods available which are being considered as standard methods of characterising the properties of porous materials. Conventional methods, such as mercury intrusion porosimetry (MIP) and gas sorption (GS), are well established but have serious disadvantages. MIP uses toxic mercury and GS is a low throughput method, in which measurements can last for several hours. Furthermore, GS cannot be applied for wet samples. Both of these methods require specialised instruments and time consuming sample preparation.

J. Riikonen · V.-P. Lehto (✉)
Department of Applied Physics, University of Eastern Finland, P.O. Box 1627, 70211 Kuopio, Finland
e-mail: vesa-pekka.lehto@uef.fi

J. Salonen
Department of Physics and Astronomy, University of Turku, 20014 Turku, Finland

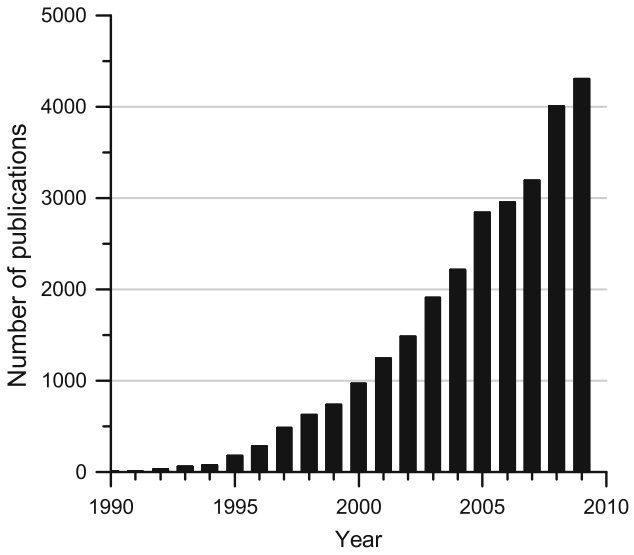

Fig. 1 The number of published papers per year (search result of a search phrase 'mesoporous or nanoporous' in ISI Web of Science)

During recent years there has been a significant development in a method called thermoporometry (TPM) (or thermoporosimetry). It is a calorimetric method of characterising properties of mesoporous materials and it is based on observation of solid–liquid phase transition in the pores. These experiments can be performed in a short time without extensive sample preparation. It is often the only available method that can be used to characterise wet samples. There is also no need for specialised instruments since thermoporometry can be performed with a common measurement instrument: differential scanning calorimeter (DSC). In fact, there are numerous porosimeters in laboratories around the world without their users realising it.

So far, thermoporometry is not being considered a standard method of characterising porous materials. Perhaps a great advantage of not needing any specialised instrument for thermoporometry has actually hindered the popularity of the method. Seemingly, commercial potential of the method has not been recognised by the instrument manufacturers and thus, it has lacked a serious promotion. So far, it has been the user's task to find the suitable equations and build the code or spreadsheets for data evaluation. We hope that this two-part review will make it easier to understand and adapt the technique for those not familiar with thermoporometry. Hopefully, we are also able to bring new insights for those scientists who are already familiar with the method.

Characterisation of mesoporous materials

Numerous methods have been developed to characterise properties of mesoporous materials such as pore volume, surface area and pore size. The most common characterisation methods are GS, MIP and electron microscopy (EM). TPM and nuclear magnetic cryoporometry (NMRC) have experienced tremendous development in recent years, making them an appealing alternative in characterisation of mesoporous materials.

Imaging

Among the common characterisation methods, EM techniques such as scanning electron microscopy (SEM) and transmission electron microscopy (TEM), are the most limited. It is impossible to calculate important parameters such as pore volume and surface area using these techniques. Although it is possible to obtain information about the pore size, it is challenging to calculate a pore size distribution (PSD) that would represent the whole sample. However, EM methods are very useful in acquiring, usually qualitative, knowledge of the pore morphology [16–18].

Mercury intrusion porosimetry

MIP is a well-established method which has been used for 70 years [19]. In these experiments, non wetting mercury is forced into the pores by applying pressure and subsequently let out of the pores by decreasing the pressure. Volume of mercury that has penetrated into the pores is recorded as a function of the applied pressure and the pore size distribution can be calculated using the Washburn equation [19, 20]

$$p = \frac{2\gamma\cos(\theta)}{r_{\mathrm{p}}} \tag{1}$$

where p is the pressure applied to mercury, γ the surface tension of mercury, r_{p} the radius of the pore and θ the contact angle between mercury and the porous material. One of the advantages of the method is that the relationship between pore size and pressure is simple and the only factor causing uncertainty in Eq. 1 is the value of the contact angle which is not always known. Another advantage is that a wide range of pores can be measured ranging from mesopores to macropores (4 nm–300 μm) [21]. It is especially used for samples exhibiting macroporosity, such as paper [22], tablets [23] and cement [24] that are difficult to measure using other methods.

Despite the evident benefits, MIP has several drawbacks, making it less appealing for routine use, especially due to toxicity of mercury. It is also susceptible to pore network effects since mercury is intruded or extruded as a continuous phase in and out of the pore network. Therefore, all pores in the pore network cannot be independently accessed by mercury. In addition, it is a destructive method since part of the mercury is easily trapped in the pores after

the experiment and the sample cannot be reused [25]. Furthermore, it is not suitable to characterise 'soft' or fragile materials as the high pressure applied on the materials might affect their pore structure [20].

Gas sorption

Gas sorption as a method to characterise porous solids dates back to early twentieth century, when it was used for surface area measurements [26]. Since mid-twentieth century it has been also used for pore size analysis [26]. It has become a standard method, and the early theories by Brunauer, Emmett and Teller (BET theory) and Barrett, Joyner and Halenda (BJH theory) are still widely used [27, 28]. In the BET theory, determination of the surface area is based on multilayer adsorption of gas on surfaces. In the BJH theory, the PSD calculation is based on the pressure dependent capillary condensation.

During a typical gas adsorption measurement the amount of adsorbed gas is recorded as function of relative pressure p/p_0 (the pressure of the gas divided by its saturation pressure) at constant temperature, yielding adsorption and desorption isotherms. Gas inside a pore experiences capillary condensation at relative pressure given by Kelvin equation. For hemispherical liquid–gas interface the Kelvin equation becomes:

$$ln\left(\frac{p}{p_0}\right) = -\frac{2\gamma_{lg}v_l}{RTr_l} \tag{2}$$

where γ_{lg} is the liquid–gas surface tension, v molar volume of the condensate, R the gas constant, T the temperature and r_l the radius of the curvature of the liquid–gas interface. The values of these constants are well known for gases typically used in the experiments, such as argon, krypton or the most commonly used nitrogen [26, 29, 30]. In addition to the conventional methods, also newer methods have been developed in order to extract porous parameters from the isotherms, such as density functional theory (DFT) which is based on theoretical calculations utilising reference adsorption isotherms [31, 32]. Not only pore size, volume and area can be deduced from the isotherms but also information about the pore morphology can be obtained. This is based on an analysis of the adsorption–desorption hysteresis [33, 34].

GS is well established method and is well suitable for characterisation of various kinds of materials often without prior knowledge of the properties of the sample. It is also a non destructive method. Even though it has been used for decades, there is still a lot of discussion about the theoretical basis of GS such as the nature of the hysteresis phenomena [35–37].

GS can be used to measure the pore sizes between 0.5 and 200 nm [37]. It is a widely used method and, therefore, its results can often be compared to those in literature. A unique feature of the GS is the possibility to independently determine the surface area of the sample without making assumptions of the pore geometry utilising the multilayer adsorption [27]. However, the main disadvantages of the method is the sample preparation requiring extensive degassing and long measurement times (hours) making it a low throughput method. GS also requires a specialised instrument for the measurements.

Methods based on solid–liquid phase transition

Characterisation methods based on solid–liquid phase transition of a confined fluid have received considerable attention during last decades. This method was pioneered by Brun et al. [38] who established the thermodynamic basis for calorimetric determination of PSD from freezing of liquid inside the pores. It is based on observation of freezing/melting of material confined in the pores as a function of temperature. The confinement of material into small pores is known to cause a depression of the melting point which is described by Gibbs–Thomson equation

$$\Delta T = T - T_0 = -\frac{\gamma_{sl}T_0}{\rho\Delta h}\frac{\mathrm{d}A}{\mathrm{d}V} = -K\frac{\mathrm{d}A}{\mathrm{d}V} \tag{3}$$

where ΔT is the melting point depression, T_0 the bulk melting temperature, γ_{sl} the surface tension of solid–liquid interface, ρ the density, Δh the specific enthalpy of melting and $\mathrm{d}A/\mathrm{d}V$ the curvature of the solid–liquid interface which is $1/r$ for cylinder and $2/r$ for sphere, where r is the radius of the curvature. K is defined as $K = \gamma_{sl}\, T_0/\rho\Delta h$.

The methods based on the observation of solid–liquid phase transition are closely related to GS methods. Both methods are based on observation of a phase transition property; capillary condensation pressure or solid–liquid phase transition temperature, which is dependent on the confinement dimensions. In both methods, liquid-like layer covers the pore walls before the phase transition. In capillary condensation, this is the adsorbed layer of molecules on the pore surface, whereas in melting it is the non-freezing δ-layer (see 'Solid state' section). The interfaces between the solid–liquid phases and liquid–gas phases are similar in both methods. For example, in a cylindrical pore the solid–liquid interface is considered to be cylindrical during melting and hemispherical during freezing. In GS the liquid–gas interface is considered to be cylindrical and hemispherical during adsorption and desorption, respectively. The main difference, in addition to the observed phase transition, is that a GS experiment is conducted isothermally as a function of pressure, whereas solid–liquid transitions are observed isobarically as a function of temperature. GS also involves mass transfer during adsorption and desorption which does not occur during freezing and

melting. Results obtained from these experiments are often consistent [39–41], although differences have also been reported [42, 43].

The use of solid–liquid transition in characterisation of porous materials is especially beneficial when studying materials whose pores are filled with liquid and whose pore structure will be affected by drying. These materials include cellulose, skin, hydrogels and mortar [44–48].

There are several methods that can be used to observe the solid–liquid phase transition in the pores as a function of temperature. The most commonly used are differential scanning calorimetry (DSC), nuclear magnetic resonance (NMR) [49–51], X-ray diffraction (XRD) [52, 53], neutron diffraction/scattering (ND) [54, 55] and dielectric spectroscopy (DS) [56, 57].

NMR cryoporometry

The technique in which NMR is utilised to probe freezing and melting of liquids in the pores to evaluate the properties of porous materials is called NMR cryoporometry (NMRC). The theory of NMR measurements in this context is beyond the scope of this review, but it is presented in other reviews [49–51]. In a typical NMRC measurement, signal intensity proportional to the total liquid volume in the sample is recorded as a function of temperature. Temperature scans are usually performed stepwise with increasing temperatures but also decreasing temperatures have been used [51, 58]. In addition to observing solid–liquid phase transition, NMR can be used in other ways to measure pore size distribution. Such methods utilise the diffusion, spin relaxation and chemical shift properties of liquids confined in pores or chemical shift of Xenon gas trapped between the frozen domains in the pores [50, 59–61].

NMRC offers several undeniable advantages; it provides information not only about melting and freezing of the confined liquid but also about the mobility of the confined molecules. This can reveal, for instance, liquid-surface interactions and diffusion of the liquid molecules [62–65]. The fact that it measures the signal from the absolute amount of liquid is advantageous since it makes it possible to increase the signal to noise ratio by simply increasing the measurement time and allows equilibrating the sample in each temperature step. It also enables good temperature resolutions and measures relatively large pores (up to 1 μm or even 10 μm) [50, 51]. Furthermore, in combination with NMR imaging, it can be used for spatial imaging of porous properties [66]. Due to these advantages, it is a valuable tool in characterising mesoporous materials, materials confined in them and their phase transitions. However, the interpretation of NMR data is not always simple. It has been reported that observed transition temperature may be strongly dependent on the delay time [67]. Also, the observed transition range in NMR does not always represent strictly pore size distribution since the possible changes of mobility in the non-freezing layer adjacent to the pore wall contribute to the signal [67]. Due to rather complicated usage of NMR and the high cost of the equipment, NMRC is unlikely to become a routine method in analysis of mesoporous materials.

Thermoporometry

In TPM, the porous properties are determined by measuring calorimetrically the solid–liquid transition in the pores. Since the pore size depends on the phase transition temperature (according to Eq. 3) and the pore volume is proportional to the melting enthalpy of the phase transition, a pore size distribution can be calculated from the DSC thermogram.

Thermoporometry has been found to be suitable for characterising vast variety of porous materials such as controlled pore glass (CPG) [68], silica gel [69], porous silicon (PSi) [70], polymer gels [71, 72], mortar [44], cellulose [47] and ordered mesoporous materials (MCM-41, SBA-15, etc.) [73–75]. Also, several materials have been used in thermoporometry to probe porous properties including water [38, 73, 76], benzene [38], acetonitrile [77], alkanes [70, 72, 78, 79], carbon tetrachloride [80–82], acetone [83] and indium [84]. However, water is the most commonly used. It is non-hazardous, readily available and its properties have been well studied. Perhaps the most important feature is the high melting enthalpy which increases the sensitivity of the experiment or makes it possible to use slower heating/cooling rates or smaller sample masses. Another advantage in using water is that water, readily adsorbed on the pore walls of hydrophilic materials from ambient air, does not contaminate the sample. However, water is known to exhibit anomalous behaviour, and even after hundreds of years of research some of its features are still controversial today [85–87].

The main advantage of thermoporometry is its simplicity. Measurements are simple and quick to perform and calculations are uncomplicated [68]. In addition, no laborious sample preparations are needed and amounts of sample used are in the order of milligrams. Despite, and also because, its simplicity it can be a powerful method in characterisation of porous materials.

A disadvantage in using DSC to measure the phase transition is that it is measuring a dynamic process of freezing or melting, and therefore, requires heating or cooling of the sample, which reduces the temperature resolution. For the same reason the sample is never in equilibrium state during a typical measurement. However, there are also reports on stepwise heating in thermoporometry,

which enables measuring the amount of frozen or melted material between two equilibrium states [88].

There are also disadvantages common for all the methods which are based on the observation of the solid–liquid phase transition of confined liquids. The main disadvantage is a requirement of calibration to establish the relation between the depression of the phase transition temperature and the pore size using samples with known pore size. The pore size of the calibration samples has to be measured by a reference method, typically by gas adsorption. This limits the accuracy of TPM to the accuracy of the reference method used in the calibration. The pore sizes that can be measured with these methods are limited to the range from few nanometres to few hundreds of nanometres. The lower limit of the pore size arises from the temperature limit where solid–liquid transition disappears and the upper pore size limit arises from the temperature resolution that enables to distinguish between the transitions that take place in the pores and in the bulk [51, 68, 89].

Confinement effects

Liquid state

A liquid confined in mesopores exhibits several features that distinguish it from the bulk. High curvature of the solid–liquid interface at the surface of the pore wall or liquid–gas interface at the pore openings causes a high pressure difference across the interface described by Young–Laplace equation

$$\Delta p = \gamma \frac{\mathrm{d}A}{\mathrm{d}V} \tag{4}$$

which is used in derivation of Kelvin equation and Gibbs–Thomson equations.

Due to the confinement, the surface area to pore volume ratio and, consequently, the fraction of molecules in contact with the pore surface, is large compared to the bulk. Therefore, interactions between the liquid molecules and the solid surface become significant. Mobility of the confined molecules has been studied using NMR, DS and neutron scattering [56, 63, 90–94]. In these studies it has been concluded that liquid in the pores exists in two or three distinguishable forms [56, 90, 93]. Liquid in the centre of the pores resembles the bulk liquid although its mobility is reduced by the confinement. Molecules on the pore walls experience interactions with the pore wall and their mobilities are further decreased. Third layer located in between the two layers has also been found with intermediate mobility [56, 93]. The mobility of the confined molecules is seen to decrease with decreasing pore size [63, 92, 95]. The temperature dependence of the mobility of the confined molecules is reported to exhibit unusual saddle-like behaviour, which was explained by the counterbalance of two competing processes: orientational fluctuations of the water molecules and the defect formation in the vicinity of water molecules [94].

Solid state

δ-*layer*

A striking feature of a pore filled with a solid substance is that between the solid core and the pore wall remains a thin non-freezing liquid layer, which we call δ-layer. In small pores, this layer can accommodate a large fraction of the confined material. This layer is of critical importance in thermoporometry as it affects both; the pore size and the pore volume calculations (see 'Calculations' section in the second part of the review [96]). In a thermoporometry experiment, this layer does not experience solid–liquid transition (as whole). However, it was estimated by Banys et al. that the water in δ-layer in the pores of MCM-41 would freeze at temperature between 21 and 26 K [56].

It is energetically favourable for the confined material to exist as a liquid on the surface of the pore [97, 98]. The formation of this layer does not require differences between molecule–molecule and molecule–wall interactions as demonstrated by Moore et al. [99]. In their simulation water was confined in 3 nm pores made of water. Despite an identical water–water and water–wall interaction, δ-layer existed between the solid core and pore wall since the liquid can accommodate the structure of the wall better than the crystal. However, when different molecule–wall interactions exist they affect the thickness of the δ-layer (δ) [100–102].

The value of δ has been determined for several liquids. For water in siliceous materials, values ranging between 0.3 and 2.6 nm have been reported, but most commonly, δ is found to be in the range from 0.5 to 0.8 nm which corresponds to two or three monolayers. [38, 67, 69, 103, 104]. Other values include 0.4 nm (2 monolayers) for argon in vycor [105], 2.1 nm (4 monolayers) for cyclohexane in silica gel [106], and 2.4 nm for carbon tetrachloride in silica gel [81]. The thickness of the δ-layer has been reported to decrease with decreasing temperature and with increasing pore curvature [54, 107].

Crystal structure

The crystal structure of the solid in pores can also be affected by the confinement. Water is reported to form cubic ice instead of the typical hexagonal ice in the mesopores [108–110]. Cubic ice is a polymorphic form of ice which does not form under normal conditions and is

metastable relative to the hexagonal form in bulk [111]. In mesopores, however, cubic ice is found to be stable before melting [112]. Structure of the cubic ice in mesopores as well as in bulk is being debated [99, 108]. Bulk cubic ice does not consist of pure cubic crystals, but there is always hexagonal ice present [112, 113]. The cubic ice in the mesopores has been suggested by Morishige and Uematsu to consist of very small hexagonal ice crystallites with disordered stacking sequence [108]. They also concluded that the probability of stacking faults decreases with increasing pore size and becomes negligible in pores with diameters larger than 100 nm. The simulation study by Moore et al. resulted in a highly defective structure having both cubic and hexagonal layers (in ratio 2 to 1, respectively) with more than three adjacent cubic or hexagonal layers being extremely rare [99]. Morishige et al. reported that the stability of the cubic ice is dependent on pore structure [112]. They found that the cubic ice was partially transformed to hexagonal ice in the interconnected spherical cavities of KIT-5 during melting, whereas cubic ice remained stable in the cylindrical, interconnected cylindrical and irregular pores of SBA-15, KIT-6 and CPG, respectively. They suggested that the difference in the stability of cubic ice is due to easier sweeping of dislocations in single crystals in spherical cavities than in the polycrystalline crystallites in the cylindrical pores. Yet, this explanation remains unclear since it has not been shown that the crystallite size in the pores would be significantly different in the different materials.

The stacking faults observed in the crystal structure of solid induced by confinement are not unique phenomena for water. Various other materials have been shown to exhibit similar stacking faults, such as krypton, xenon, argon and gallium [114–118]. Changes in the crystal form induced by confinement have also been reported with other materials than water. Previously unknown polymorphs have been reported to form under confinement [118, 119]. In addition, a change in the stability order between polymorphs and transition from enantiotropic into monotropic behaviour was found with organic molecules [119]. It has also been reported that confinement can influence the spatial ordering in the crystals of linear alkanes and that tortuosity of the pores could suppress their lamellar ordering [120, 121].

Solid–liquid phase transition

Melting and freezing

Melting of a confined solid can proceed in two ways. It can be initiated from the surface of the pores and proceed radially towards the centre of the pore. This kind of melting was described already by Brun et al. and has been later reformulated by several authors [84, 98, 105, 122]. Other possibility is that melting is initiated at high energy locations or at closed end in the pore and propagates along the pore axis [40].

There are also two ways freezing can occur. Crystallisation in the pores can take place by heterogeneous nucleation from macroscopic crystals outside the pores or inside the adjacent pore that has already been frozen [38]. If no nucleation centres are present, the pore liquid will freeze by homogenous nucleation [42]. It is important to distinguish between the two situations where external solid phase is or is not present outside the pores to act as nucleation centres. It has been observed that if no solid phase is present outside the pores, freezing temperature in the pores is lowered and the freezing curve in thermoporometry or NMR cryoporometry does not represent the PSD of the sample [73].

Freezing and melting in partially filled pores presents interesting phenomena which have been reported by several authors [73, 105, 123]. Wallacher and Knorr presented a comprehensive study of freezing of argon in the pores of Vycor glass using different degrees of pore filling. They concluded that there are two monolayers of argon on the surface of the pores (i.e. δ-layer) that do not take part in the phase transition. The layers above δ-layer in the incompletely filled pores can delayer and form crystals at the centre of the pores. The delayering takes place at lower temperatures compared to the freezing of liquid argon at the centre of the pores. Melting, however, took place at the same temperature weather the frozen argon was originally from the adsorbed layer or pore centres, proving that the delayered argon solidifies at the centre of the pores. Similar data was published almost simultaneously by Schreiber et al. describing freezing and melting of water in incompletely filled pores of SBA-15 [73]. The concept of delayering was also adapted in this case with the difference that two delayering temperatures were clearly observed instead of one associated with the delayering of different monolayers [39].

In some, rather rare, systems the confinement can result in elevation of the solid–liquid phase transition [124–128]. This is attributed to very strong wall–liquid interactions, which exceed liquid–liquid interactions [128].

Confinement also affects other transitions than the solid–liquid and liquid–gas transitions. It has been stated that confinement can increase or decrease the glass transition temperature or it can also remain unchanged [129]. It has been also shown that solid–solid transitions temperatures are depressed due to the confinement [80, 130, 131]. Baba et al. demonstrated that solid–solid transition temperature of cyclohexane can be used in thermoporometry to measure the pore size [79].

Melting–freezing hysteresis

Melting and freezing of materials in mesopores is known to exhibit hysteretic behaviour, i.e. freezing in the pores is observed at lower temperatures compared to melting. The reason behind the melting–freezing hysteresis has been suggested to be, e.g. different shapes of solid–liquid interface, pore blocking effect, free energy barrier in melting, and nucleation during freezing [38, 40, 42, 98].

The nature of the capillary freezing and melting, and consequently the reason for freezing–melting hysteresis, is widely debated [38, 39, 67, 98, 105, 122, 132, 133]. It has not been yet established weather the melting or freezing in confinement (or neither of them) takes place at equilibrium temperature. The equilibrium temperature is the temperature at which the free energies of the solid and liquid in the pores are equal.

The theories, based on the evaluation of free energy of a system as a function of radius of the solid core in the pores, describe the melting to occur at metastable state [84, 98, 122]. According to these theories, metastability exists because the shrinking of the solid core in the pore requires surmounting an energy barrier. Therefore, melting takes place at elevated temperatures at which the energy barrier becomes lower. Freezing is treated as an equilibrium transition due to the nucleation at the solid outside the pores and subsequent penetration of the solid–liquid interface which does not require a change of shape of the interface.

However, as pointed out by Morishige et al. [40], there is a discrepancy between the free energy model and the experiments. The calculated melting temperature for solid in cylindrical pores would be $\Delta T_m = -K/r_s$ according to the free energy model [98]. This is in contradiction with the experimental melting point depression of water in the cylindrical pores of MCM-41 and SBA-15 which has been found to follow closely Gibbs–Thomson equation (Eq. 3) $\Delta T_m = -2\,K/r_s$, where the curvature of solid–liquid interface is $2/r_s$, i.e. hemispherical surface [67, 73].

Wallacher and Knorr, who derived similar free energy theory as the theories mentioned before, concluded that superheating of pore solid is irrelevant. The conclusion was based on adaption of varying pore geometries, such as pores with one closed end, in which melting would take place through axial propagation of the solid–liquid interface in the pore network [105]. Therefore, they suggested that the liquid is in a metastable state during freezing.

Kondrashova et al. performed NMRC measurements using nitrobenzene in Vycor where the freezing and melting transitions were observed by reversing the heating or cooling scan upon incomplete transition [133]. They concluded that their study did not support equilibrium freezing, since freezing was observed at higher temperatures if there was solid phase present in the pores compared to the scan started from completely liquid state.

In conclusion, it seems that without challenging the validity of the free energy model itself, the real porous materials and the confined solids in them are not homogenous enough so that the metastable surface melting phenomena would have considerable effect. Even solids in the ordered mesoporous materials, such as MCM-41 and SBA-15, which are considered to be the best models for cylindrical pores, seem to have sufficient amount of high energy sections that can initiate melting. Melting then proceeds by propagation of a solid–liquid front along the pore axis. Therefore, the solid in the pores would melt at considerably lower temperatures than predicted by the surface melting in the free energy models.

Supercooling of liquid is known to occur in the pores if there is no solid phase outside the pores to nucleate the freezing due to the kinetics of nucleation [73]. It is also well understood that the pore blocking will lead to supercooling in part of the pore network [42, 134]. In the pore blocking, larger pores are isolated by smaller pores, and therefore, the larger pore will freeze only when the temperature is low enough for the solid phase to proceed through the narrow pores and provide a nucleation centre to the larger pore. It is possible that the homogenous nucleation takes place in the larger pores isolated by smaller pores, but at this stage the liquid in the larger pores is already substantially undercooled [42].

However, it is unclear why liquid in the pores is supercooled beyond the equilibrium temperature when there is a solid phase outside the pores and the pores are expected to consist of uniform cylindrical pores as in MCM-41. It was suggested that the freezing temperature is lowered due to incompatibility of hexagonal ice outside the pores and cubic ice in the pores [73]. It has also been suggested that even for the ordered mesoporous materials, constrictions at the pores entrances occur limiting the size of the penetrating crystallites [39, 67]. It is indeed possible that the same kind of heterogeneity of the pores that initiate melting in the pores is responsible for the hindering the penetration of the solid front, and therefore, lowering the freezing temperature.

Hysteresis width (the temperature difference between melting and freezing) has been found to narrow, and eventually disappear, as pore size is decreased [73, 132]. A reason for this has been suggested to be the lowering of the free energy barrier in the case of melting with decreasing pore size [98, 122]. Another explanation was given by Jähnert et al. [67], who suggested that below the critical pore size 2.9 nm, the freezing of water does not occur as a true first order phase transition due to similarity of the solid and liquid phases. This was explained by the increasing disorder of the ice with decreasing pore size and, on the

other hand, by the increasing short-range ordering of the liquid phase with decreasing temperature. Their conclusion is supported by X-ray diffraction (XRD) and neutron diffraction studies of the ice under confinement as well as NMR and FTIR studies of confined water [53, 135–138]. Further support was provided by their observation that melting enthalpy of confined water is also decreasing as pore size decreases, even when the effect of δ-layer is taken into account. It was extrapolated that the melting enthalpy would diminish in pores with diameter under 2.7 nm, close to the pore size in which the hysteresis disappears.

Conclusions

Thermoporometry is a powerful method of characterising mesoporous materials and it has many advantages over the conventional methods. Measurements are possible to conduct in a short time without toxic chemicals and the sample preparation is simple. Thermoporometry is one of the few available methods to characterise wet samples and there is no need for specialised instruments, since a DSC can be used to perform the measurements.

The confinement effects on freezing and melting in porous materials have been widely studied in recent decades and providing new information about this interesting phenomenon. However, several questions remain unanswered about the nature of solid–liquid phase transition under confinement.

Acknowledgements The financial support from the Academy of Finland (grant no. 118002 and 122314) is acknowledged.

References

1. Davis ME. Ordered porous materials for emerging applications. Nature. 2002;417:813–21.
2. Ciesla U, Schüth F. Ordered mesoporous materials. Microporous Mesoporous Mater. 1999;27:131–49.
3. Taguchi A, Schüth F. Ordered mesoporous materials in catalysis. Microporous Mesoporous Mater. 2005;77:1–45.
4. Parkhutik V. Porous silicon—mechanisms of growth and applications. Solid-State Electron. 1999;43:1121–41.
5. Jalkanen T, Torres-Costa V, Salonen J, Bjorkqvist M, Makila E, Martinez-Duart JM, Lehto V. Optical gas sensing properties of thermally hydrocarbonized porous silicon bragg reflectors. Opt Express. 2009;17:5446–56.
6. Torres-Costa V, Martín-Palma RJ. Application of nanostructured porous silicon in the field of optics. A review. J Mater Sci. 2010;45:2823–38.
7. Salonen J, Kaukonen A, Hirvonen J, Lehto V. Mesoporous silicon in drug delivery applications. J Pharm Sci. 2008;97:632–53.
8. Jane A, Dronov R, Hodges A, Voelcker NH. Porous silicon biosensors on the advance. Trends Biotechnol. 2009;27:230–9.
9. Salonen J, Laitinen L, Kaukonen A, Tuura J, Björkqvist M, Heikkilä T, Vähä-Heikkilä K, Hirvonen J, Lehto V. Mesoporous silicon microparticles for oral drug delivery: loading and release of five model drugs. J Control Release. 2005;108:362–74.
10. Heikkilä T, Salonen J, Tuura J, Kumar N, Salmi T, Murzin DY, Hamdy MS, Mul G, Laitinen L, Kaukonen A, Hirvonen J, Lehto V. Evaluation of mesoporous TCPSi, MCM-41, SBA-15, and TUD-1 materials as API carriers for oral drug delivery. Drug Deliv. 2007;15:337–47.
11. Kilpeläinen M, Riikonen J, Vlasova MA, Huotari A, Lehto V, Salonen J, Herzig KH, Järvinen K. In vivo delivery of a peptide, ghrelin antagonist, with mesoporous silicon microparticles. J Control Release. 2009;137:166–70.
12. Canham L. Properties of porous silicon. London: The Institution of Electrical Engineers; 1997.
13. Zhao DY, Huo QS, Feng JL, Chmelka BF, Stucky GD. Nonionic triblock and star diblock copolymer and oligomeric surfactant syntheses of highly ordered, hydrothermally stable, mesoporous silica structures. J Am Chem Soc. 1998;120:6024–36.
14. Kresge CT, Leonowicz ME, Roth WJ, Vartuli JC, Beck JS. Ordered mesoporous molecular-sieves synthesized by a liquid-crystal template mechanism. Nature. 1992;359:710–2.
15. Kleitz F, Liu D, Anilkumar GM, Park I-S, Solovyov LA, Shmakov AN, Ryoo R. Large cage face-centered-cubic Fm3m mesoporous silica: synthesis and structure. J Phys Chem B. 2003;107:14296–300.
16. Endo A, Yamada M, Kataoka S, Sano T, Inagi Y, Miyaki A. Direct observation of surface structure of mesoporous silica with low acceleration voltage FE-SEM. Colloids Surf A. 2010;357:11–6.
17. Che SN, Lund K, Tatsumi T, Iijima S, Joo SH, Ryoo R, Terasaki O. Direct observation of 3D mesoporous structure by scanning electron microscopy (SEM): SBA-15 silica and CMK-5 carbon. Angew Chem Int Ed Engl. 2003;42:2182–5.
18. Thiruvengadathan R, Levi-Kalisman Y, Regev O. Templating nanostructures by mesoporous materials with an emphasis on room temperature and cryogenic TEM studies. Curr Opin Colloid Interface Sci. 2005;10:280–6.
19. Van Brakel J, Modrý S, Svatá M. Mercury porosimetry: state of the art. Powder Technol. 1981;29:1–12.
20. Léon Y, León CA. New perspectives in mercury porosimetry. Adv Colloid Interface Sci. 1998;76–77:341–72.
21. Porcheron F, Monson PA, Thommes M. Modeling mercury porosimetry using statistical mechanics. Langmuir. 2004;20:6482–9.
22. Johnson RW, Abrams L, Maynard RB, Amick TJ. Use of mercury porosimetry to characterize pore structure and model end-use properties of coated papers. Part I: optical and strength properties. Tappi J. 1999;82:239–51.
23. Wikberg M, Alderborn G. Compression characteristics of granulated materials. VI: pore size distributions, assessed by mercury penetration, of compacts of two lactose granulations with different fragmentation propensities. Int J Pharm. 1992;84:191–5.
24. Cook RA, Hover KC. Mercury porosimetry of hardened cement pastes. Cem Concr Res. 1999;29:933–43.
25. Denoyel R, Llewellyn P, Beurroies I, Rouquerol J, Rouquerol FO, Luciani L. Comparing the basic phenomena involved in three methods of pore-size characterization: gas adsorption, liquid intrusion and thermoporometry. Part Part Syst Charact. 2004;21:128.
26. Sing K. The use of nitrogen adsorption for the characterisation of porous materials. Colloids Surf A. 2001;187-188:3–9.
27. Brunauer S, Emmett PH, Teller E. Adsorption of gases in multimolecular layers. J Am Chem Soc. 1938;60:309–19.

28. Barrett EP, Joyner LG, Halenda PP. The determination of pore volume and area distributions in porous substances. 1. Computations from nitrogen isotherms. J Am Chem Soc. 1951;73: 373–80.
29. Thommes M, Köhn R, Früba M. Sorption and pore condensation behavior of nitrogen, argon, and krypton in mesoporous MCM-48 silica materials. J Phys Chem B. 2000;104:7932–43.
30. Kruk M, Jaroniec M. Gas adsorption characterization of ordered organic–inorganic nanocomposite materials. Chem Mater. 2001; 13:3169–83.
31. Tarazona P, Marconi UMB, Evans R. Phase-equilibria of fluid interfaces and confined fluids—nonlocal versus local density functionals. Mol Phys. 1987;60:573–95.
32. Neimark AV, Ravikovitch PI. Capillary condensation in MMS and pore structure characterization. Microporous Mesoporous Mater. 2001;44–45:697–707.
33. Seaton NA. Determination of the connectivity of porous solids from nitrogen sorption measurements. Chem Eng Sci. 1991;46: 1895–909.
34. Morishige K, Tateishi N. Adsorption hysteresis in ink-bottle pore. J Chem Phys. 2003;119:2301–6.
35. Morishige K. Adsorption hysteresis in ordered mesoporous silicas. Adsorption. 2008;14:157–63.
36. Liu H, Zhang L, Seaton NA. Sorption hysteresis as a probe of pore structure. Langmuir. 1993;9:2576–82.
37. Groen JC, Peffer LAA, Pérez-Ramírez J. Pore size determination in modified micro- and mesoporous materials. Pitfalls and limitations in gas adsorption data analysis. Microporous Mesoporous Mater. 2003;60:1–17.
38. Brun M, Lallemand A, Quinson J, Eyraud C. A new method for simultaneous determination of size and shape of pores: the thermoporometry. Thermochim Acta. 1977;21:59–88.
39. Findenegg GH, Jaehnert S, Akcakayiran D, Schreiber A. Freezing and melting of water confined in silica nanopores. ChemPhysChem. 2008;9:2651–9.
40. Morishige K, Yasunaga H, Matsutani Y. Effect of pore shape on freezing and melting temperatures of water. J Phys Chem C. 2010;114:4028–35.
41. Beurroies I, Denoyel R, Llewellyn P, Rouquerol J. A comparison between melting-solidification and capillary condensation hysteresis in mesoporous materials: application to the interpretation of thermoporometry data. Thermochim Acta. 2004;421:11–8.
42. Morishige K, Yasunaga H, Denoyel R, Wernert V. Pore-blocking-controlled freezing of water in cagelike pores of KIT-5. J Phys Chem C. 2007;111:9488–95.
43. Riikonen J, Salonen J, Kemell M, Kumar N, Murzin DY, Ritala M, Lehto V. A novel method of quantifying the u-shaped pores in SBA-15. J Phys Chem C. 2009;113:20349–54.
44. Sun Z, Scherer GW. Pore size and shape in mortar by thermoporometry. Cem Concr Res. 2010;40:740–51.
45. Fathima NN, Kumar MP, Rao JR, Nair BU. A DSC investigation on the changes in pore structure of skin during leather processing. Thermochim Acta. 2010;501:98–102.
46. Chan AW, Neufeld RJ. Modeling the controllable pH-responsive swelling and pore size of networked alginate based biomaterials. Biomaterials. 2009;30:6119–29.
47. Luukkonen P, Maloney T, Rantanen J, Paulapuro H, Yliruusi J. Microcrystalline cellulose–water interaction—a novel approach using thermoporosimetry. Pharm Res. 2001;18:1562–9.
48. Książczak A, Gołofit T, Tomaszewski W. Binary system nitrocellulose from linters + sym-diethyldiphenylurea: thermal analysis of phase transition and pore structure. J Therm Anal Calorim. 2008;91:375–80.
49. Webber JBW. Studies of nano-structured liquids in confined geometries and at surfaces. Prog Nucl Magn Reson Spectrosc. 2010;56:78–93.
50. Petrov OV, Furó I. NMR cryoporometry: principles, applications and potential. Prog Nucl Magn Reson Spectrosc. 2009; 54:97–122.
51. Mitchell J, Webber JBW, Strange JH. Nuclear magnetic resonance cryoporometry. Phys Rep. 2008;461:1–36.
52. Morishige K, Nobuoka K. X-ray diffraction studies of freezing and melting of water confined in a mesoporous adsorbent (MCM-41). J Chem Phys. 1997;107:6965–9.
53. Morishige K, Iwasaki H. X-ray study of freezing and melting of water confined within SBA-15. Langmuir. 2003;19:2808–11.
54. Liu E, Dore JC, Webber JBW, Khushalani D, Jähnert S, Findenegg GH, Hansen T. Neutron diffraction and NMR relaxation studies of structural variation and phase transformations for water/ice in SBA-15 silica. I: the over-filled case. J Phys. 2006;18:10009–28.
55. Jelassi J, Castricum HL, Bellissent-Funel M-, Dore J, Webber JBW, Sridi-Dorbez R. Studies of water and ice in hydrophilic and hydrophobic mesoporous silicas: pore characterisation and phase transformations. Phys Chem Chem Phys. 2010;12: 2838–49.
56. Banys J, Kinka M, MacUtkevic J, Völkel G, Böhlmann W, Umamaheswari V, Hartmann M, Pöppl A. Broadband dielectric spectroscopy of water confined in MCM-41 molecular sieve materials—low-temperature freezing phenomena. J Phys. 2005;17:2843–57.
57. Sliwinska-Bartkowiak M, Dudziak G, Sikorski R, Gras R, Radhakrishnan R, Gubbins KE. Melting/freezing behavior of a fluid confined in porous glasses and MCM-41: dielectric spectroscopy and molecular simulation. J Chem Phys. 2001; 114:950–62.
58. Petrov OV, Furó I. A joint use of melting and freezing data in NMR cryoporometry. Microporous Mesoporous Mater. 2010; 136:83–91.
59. Telkki V-V, Lounila J, Jokisaari J. Behavior of acetonitrile confined to mesoporous silica gels as studied by ^{129}Xe NMR: a novel method for determining the pore sizes. J Phys Chem B. 2005;109:757–63.
60. Watson AT, Chang CTP. Characterizing porous media with NMR methods. Prog Nucl Magn Reson Spectrosc. 1997;31:343–86.
61. Barrie PJ, Klinowski J. ^{129}Xe NMR as a probe for the study of microporous solids: a critical review. Prog Nucl Magn Reson Spectrosc. 1992;24:91–108.
62. Perkins EL, Lowe JP, Edler KJ, Tanko N, Rigby SP. Determination of the percolation properties and pore connectivity for mesoporous solids using NMR cryodiffusometry. Chem Eng Sci. 2008;63:1929–40.
63. Hwang DW, Chu C-C, Sinha AK, Hwang L-P. Dynamics of supercooled water in various mesopore sizes. J Chem Phys. 2007;126:044702.
64. Gun'ko VM, Turov VV, Bogatyrev VM, Zarko VI, Leboda R, Goncharuk EV, Novza AA, Turov AV, Chuiko AA. Unusual properties of water at hydrophilic/hydrophobic interfaces. Adv Colloid Interface Sci. 2005;118:125–72.
65. Sklari S, Rahiala H, Stathopoulos V, Rosenholm J, Pomonis P. The influence of surface acid density on the freezing behavior of water confined in mesoporous MCM-41 solids. Microporous Mesoporous Mater. 2001;49:1–13.
66. Strange JH, Webber JBW. Spatially resolved pore size distributions by NMR. Meas Sci Technol. 1997;8:555–61.
67. Jähnert S, Vaca Chávez F, Schaumann GE, Schreiber A, Schönhoff M, Findenegg GH. Melting and freezing of water in cylindrical silica nanopores. Phys Chem Chem Phys. 2008;10:6039–51.
68. Landry MR. Thermoporometry by differential scanning calorimetry: experimental considerations and applications. Thermochim Acta. 2005;433:27.

69. Ishikiriyama K, Todoki M, Motomura K. Pore-size distribution (PSD) measurements of silica-gels by means of differential scanning calorimetry. I: optimization for determination of PSD. J Colloid Interface Sci. 1995;171:92.
70. Faivre C, Bellet D, Dolino G. Phase transitions of fluids confined in porous silicon: a differential calorimetry investigation. Eur Phys J B. 1999;7:19–36.
71. Baba M, Gardette J-, Lacoste J. Crosslinking on ageing of elastomers. II. Comparison of solvent freezing point depression and conventional crosslinking evaluation. Polym Degrad Stab. 1999;65:415–20.
72. Baba M, Nedelec J-, Lacoste J, Gardette J-, Morel M. Crosslinking of elastomers resulting from ageing: use of thermoporosimetry to characterise the polymeric network with *n*-heptane as condensate. Polym Degrad Stab. 2003;80:305–13.
73. Schreiber A, Ketelsen I, Findenegg GH. Melting and freezing of water in ordered mesoporous silica materials. Phys Chem Chem Phys. 2001;3:1185.
74. Kloetstra KR, Zandbergen HW, van Koten MA, van Bekkum H. Thermoporometry as a new tool in analyzing mesoporous MCM-41 materials. Catal Lett. 1995;33:145.
75. Yamamoto T, Endo A, Inagi Y, Ohmori T, Nakaiwa M. Evaluation of thermoporometry for characterization of mesoporous materials. J Colloid Interface Sci. 2005;284:614.
76. Ishikiriyama K, Todoki M. Pore-size distribution measurements of silica-gels by means of differential scanning calorimetry. II. Thermoporosimetry. J Colloid Interface Sci. 1995;171:103–11.
77. Wulff M. Pore size determination by thermoporometry using acetonitrile. Thermochim Acta. 2004;419:291–4.
78. Bahloul N, Baba M, Nedelec J-M. Universal behavior of linear alkanes in a confined medium: toward a calibrationless use of thermoporometry. J Phys Chem B. 2005;109:16227–9.
79. Baba M, Nedelec J-M, Lacoste J, Gardette J-L. Calibration of cyclohexane solid–solid phase transition thermoporosimetry and application to the study of crosslinking of elastomers upon aging. J Non-Cryst Solids. 2003;315:228–38.
80. Takei T, Onoda Y, Fuji M, Watanabe T, Chikazawa M. Anomalous phase transition behavior of carbon tetrachloride in silica pores. Thermochim Acta. 2000;352–353:199–204.
81. Husár B, Commereuc S, Lukáč I, Chmela Š, Nedelec JM, Baba M. Carbon tetrachloride as a thermoporometry liquid probe to study the cross-linking of styrene copolymer networks. J Phys Chem B. 2006;110:5315–20.
82. Meziane A, Grolier J-E, Baba M, Nedelec J-. Crystallization of carbon tetrachloride in confined geometries. Faraday Discuss. 2007;136:383–94.
83. Nedelec J-M, Grolier J-E, Baba M. Thermoporosimetry: a powerful tool to study the cross-linking in gels networks. J Sol Gel Sci Technol. 2006;40:191–200.
84. Unruh KM, Huber TE, Huber CA. Melting and freezing behavior of indium metal in porous glasses. Phys Rev B. 1993;48:9021–7.
85. Johari GP. Water's character from dielectric relaxation above its T_g. J Chem Phys. 1996;105:7079–82.
86. Mishima O, Stanley HE. The relationship between liquid, supercooled and glassy water. Nature. 1998;396:329–35.
87. Debenedetti PG. Supercooled and glassy water. J Phys. 2003;15:R1669–726.
88. Gane PAC, Ridgway CJ, Lehtinen E, Valiullin R, Furó I, Schoelkopf J, Paulapuro H, Daicic J. Comparison of NMR cryoporometry, mercury intrusion porosimetry, and DSC thermoporosimetry in characterizing pore size distributions of compressed finely ground calcium carbonate structures. Ind Eng Chem Res. 2004;43:7920–7.
89. Barrande M, Beurroies I, Denoyel R, Tatárová I, Gramblička M, Polakovič M, Joehnck M, Schulte M. Characterisation of porous materials for bioseparation. J Chromatogr A. 2009;1216:6906–16.
90. Overloop K, Vangerven L. Exchange and cross-relaxation in adsorbed water. J Magn Reson. 1993;101:147–56.
91. Overloop K, van Gerven L. NMR relaxation in adsorbed water. J Magn Reson. 1992;100:303–15.
92. Takahara S, Nakano M, Kittaka S, Kuroda Y, Mori T, Hamano H, Yamaguchi T. Neutron scattering study on dynamics of water molecules in MCM-41. J Phys Chem B. 1999;103:5814–9.
93. Hwang DW, Sinha AK, Cheng C-Y, Yu T-Y, Hwang L-P. Water dynamics on the surface of MCM-41 via ^{2}H double quantum filtered NMR and relaxation measurements. J Phys Chem B. 2001;105:5713–21.
94. Frunza L, Kosslick H, Pitsch I, Frunza S, Schönhals A. Rotational fluctuations of water inside the nanopores of SBA-type molecular sieves. J Phys Chem B. 2005;109:9154–9.
95. Takamuku T, Yamagami M, Wakita H, Masuda Y, Yamaguchi T. Thermal property, structure, and dynamics of supercooled water in porous silica by calorimetry, neutron scattering, and NMR relaxation. J Phys Chem B. 1997;101:5730–9.
96. Riikonen J, Salonen J, Lehto V. Utilising thermoporometry to obtain new insights into nanostructured materials—review part 2. J Therm Anal Calorim. 2010.
97. Pellenq RJ-, Coasne B, Denoyel RO, Coussy O. Simple phenomenological model for phase transitions in confined geometry. 2. Capillary condensation/evaporation in cylindrical mesopores. Langmuir. 2009;25:1393–402.
98. Petrov O, Furó I. Curvature-dependent metastability of the solid phase and the freezing–melting hysteresis in pores. Phys Rev E. 2006;73:011608-1–7.
99. Moore EB, De La Llave E, Welke K, Scherlis DA, Molinero V. Freezing, melting and structure of ice in a hydrophilic nanopore. Phys Chem Chem Phys. 2010;12:4124–34.
100. Turov VV, Mironyuk IF. Adsorption layers of water on the surface of hydrophilic, hydrophobic and mixed silicas. Colloids Surf A. 1998;134:257–63.
101. Turov VV, Leboda R. Application of ^{1}H NMR spectroscopy method for determination of characteristics of thin layers of water adsorbed on the surface of dispersed and porous adsorbents. Adv Colloid Interface Sci. 1999;79:173–211.
102. Riikonen J, Mäkilä E, Salonen J, Lehto V. Determination of physical state of drug molecules in mesoporous silicon with different surface chemistries. Langmuir. 2009;25:6137–42.
103. Hansen EW, Stöcker M, Schmidt R. Low-temperature phase transition of water confined in mesopores probed by NMR. Influence on pore size distribution. J Phys Chem. 1996;100:2195–200.
104. Endo A, Yamamoto T, Inagi Y, Wakabe K, Ohmori T. Characterization of nonfreezable pore water in mesoporous silica by thermoporometry. J Phys Chem C. 2008;112:9034–9.
105. Wallacher D, Knorr K. Melting and freezing of ar in nanopores. Phys Rev B. 2001;63:104202.
106. Amanuel S, Bauer H, Bonventre P, Lasher D. Nonfreezing interfacial layers of cyclohexane in nanoporous silica. J Phys Chem C. 2009;113:18983–6.
107. Petrov OV, Vargas-Florencia D, Furó I. Surface melting of octamethylcyclotetrasiloxane confined in controlled pore glasses: curvature effects observed by ^{1}NMR. J Phys Chem B. 2007;111:1574–81.
108. Morishige K, Uematsu H. The proper structure of cubic ice confined in mesopores. J Chem Phys. 2005;122:1–4.
109. Steytler DC, Dore JC, Wright CJ. Neutron diffraction study of cubic ice nucleation in a porous silica network. J Phys Chem. 1983;87:2458–9.
110. Bellissent-Funel M-C, Lal J, Bosio L. Structural study of water confined in porous glass by neutron scattering. J Chem Phys. 1993;98:4246–52.

111. Mayer E, Hallbrucker A. Cubic ice from liquid water. Nature. 1987;325:601–2.
112. Morishige K, Yasunaga H, Uematsu H. Stability of cubic ice in mesopores. J Phys Chem C. 2009;113:3056–61.
113. Bertie JE, Jacobs SM. Far-infrared absorption by ices ih and ic at 4.3°K and the powder diffraction pattern of ice ic. J Chem Phys. 1977;67:2445–8.
114. Brown DW, Sokol PE, Ehrlich SN. New disorder induced phase transitions of classical rare gases in porous vycor glass. Phys Rev Lett. 1998;81:1019–22.
115. Schäfer B, Balszunat D, Langel W, Asmussen B. Contrast X-ray powder diffraction of solid rare gas nanocrystals in silica gel mesopores. Mol Phys. 1996;89:1057–70.
116. Huber P, Knorr K. Adsorption-desorption isotherms and X-ray diffraction of ar condensed into a porous glass matrix. Phys Rev B. 1999;60:12657–65.
117. Christenson HK. Confinement effects on freezing and melting. J Phys. 2001;13:R95–133.
118. Lee MK, Tien C, Charnaya EV, Sheu H-S, Kumzerov YA. Structural variations in nanosized confined gallium. Phys Lett A. 2010;374:1570–3.
119. Ha JM, Hamilton BD, Hillmyer MA, Ward MD. Phase behavior and polymorphism of organic crystals confined within nanoscale chambers. Cryst Growth Des. 2009;9:4766–77.
120. Huber P, Wallacher D, Albers J, Knorr K. Quenching of lamellar ordering in an *n*-alkane embedded in nanopores. Europhys Lett. 2004;65:351–7.
121. Henschel A, Hofmann T, Huber P, Knorr K. Preferred orientations and stability of medium length *n*-alkanes solidified in mesoporous silicon. Phys Rev E. 2007;75:021607.
122. Denoyel R, Pellenq RJM. Simple phenomenological models for phase transitions in a confined geometry. 1. Melting and solidification in a cylindrical pore. Langmuir. 2002;18:2710–6.
123. Tombari E, Ferrari C, Salvetti G, Johari GP. Dynamic and apparent specific heats during transformation of water in partly filled nanopores during slow cooling to 110 K and heating. Thermochim Acta. 2009;492:37–44.
124. Radhakrishnan R, Gubbins KE, Watanabe A, Kaneko K. Freezing of simple fluids in microporous activated carbon fibers: comparison of simulation and experiment. J Chem Phys. 1999;111:9058–67.
125. Zhang D, Tian S, Xiao D. Experimental study on the phase change behavior of phase change material confined in pores. Sol Energy. 2007;81:653–60.
126. Radhakrishnan R, Gubbins KE. Free energy studies of freezing in slit pores: an order-parameter approach using Monte Carlo simulation. Mol Phys. 1999;96:1249–67.
127. Maheshwari P, Dutta D, Sharma SK, Sudarshan K, Pujari PK, Majumder M, Pahari B, Bandyopadhyay B, Ghoshray K, Ghoshray A. Effect of interfacial hydrogen bonding on the freezing/melting behavior of nanoconfined liquids. J Phys Chem C. 2010;114:4966–72.
128. Coasne B, Czwartos J, Sliwinska-Bartkowiak M, Gubbins KE. Effect of pressure on the freezing of pure fluids and mixtures confined in nanopores. J Phys Chem B. 2009;113:13874–81.
129. Alcoutlabi M, McKenna GB. Effects of confinement on material behaviour at the nanometre size scale. J Phys. 2005;17: R461–524.
130. Awschalom DD, Warnock J. Supercooled liquids and solids in porous glass. Phys Rev B. 1987;35:6779–85.
131. Mu R, Malhotra VM. Effects of surface and physical confinement on the phase transitions of cyclohexane in porous silica. Phys Rev B. 1991;44:4296–303.
132. Morishige K, Kawano K. Freezing and melting of water in a single cylindrical pore: the pore-size dependence of freezing and melting behavior. J Chem Phys. 1999;110:4867–72.
133. Kondrashova D, Reichenbach C, Valiullin R. Probing pore connectivity in random porous materials by scanning freezing and melting experiments. Langmuir. 2010;26:6380–5.
134. Dvoyashkin M, Khokhlov A, Valiullin R, Kärger J. Freezing of fluids in disordered mesopores. J Chem Phys 2008;129: 154702–6.
135. Dore J. Structural studies of water in confined geometry by neutron diffraction. Chem Phys. 2000;258:327–47.
136. Tanaka H. A new scenario of the apparent fragile-to-strong transition in tetrahedral liquids: water as an example. J Phys. 2003;15:L703–11.
137. Mallamace F, Broccio M, Corsaro C, Faraone A, Majolino D, Venuti V, Liu L, Mou C-Y, Chen S-H. Evidence of the existence of the low-density liquid phase in supercooled, confined water. Proc Natl Acad Sci USA. 2007;104:424–8.
138. Mallamace F, Branca C, Broccio M, Corsaro C, Mou C-Y, Chen S-H. The anomalous behavior of the density of water in the range 30 K $< T <$ 373 K. Proc Natl Acad Sci USA. 2007; 104:18387–91.